mAbs

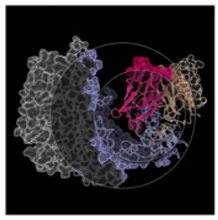

ISSN: 1942-0862 (Print) 1942-0870 (Online) Journal homepage: www.tandfonline.com/journals/kmab20

Translational minimal physiologically based pharmacokinetic model for transferrin receptor-mediated brain delivery of antibodies

Morris Muliaditan, Tamara J. van Steeg, Lindsay B. Avery, Wei Sun, Timothy R. Hammond, Diana Hijdra, Siak-Leng Choi, Nikhil Pillai, Nina C. Leksa & Panteleimon D. Mavroudis

To cite this article: Morris Muliaditan, Tamara J. van Steeg, Lindsay B. Avery, Wei Sun, Timothy R. Hammond, Diana Hijdra, Siak-Leng Choi, Nikhil Pillai, Nina C. Leksa & Panteleimon D. Mavroudis (2025) Translational minimal physiologically based pharmacokinetic model for transferrin receptor-mediated brain delivery of antibodies, mAbs, 17:1, 2515414, DOI: 10.1080/19420862.2025.2515414

To link to this article: https://doi.org/10.1080/19420862.2025.2515414

MABS
2025, VOL. 17, NO. 1, 2515414
https://doi.org/10.1080/19420862.2025.2515414

Taylor & Francis
Taylor & Francis Group

REPORT

Translational minimal physiologically based pharmacokinetic model for transferrin receptor-mediated brain delivery of antibodies

Morris Muliaditan[a], Tamara J. van Steeg[a], Lindsay B. Avery[b], Wei Sun[b], Timothy R. Hammond[c], Diana Hijdra[a], Siak-Leng Choi[d], Nikhil Pillai[e], Nina C. Leksa[c], and Panteleimon D. Mavroudis[e]

[a]Leiden Experts on Advanced Pharmacokinetics and Pharmacodynamics (LAP&P), Leiden, The Netherlands; [b]Sanofi, Quantitative Pharmacology-Innovation, Cambridge, MA, USA; [c]Sanofi, Rare and Neurologic Diseases, Cambridge, MA, USA; [d]Sanofi, Quantitative Pharmacology-Pharmacometrics, Vitry-Sur-Seine, France; [e]Sanofi, Quantitative Pharmacology-Pharmacometrics, Cambridge, MA, USA

ABSTRACT

Successful development of monoclonal antibodies (mAbs) for the treatment of central nervous system disorders has been challenging due to their minimal ability to cross the blood–brain barrier (BBB), resulting in poor brain exposure. Bispecific antibodies (bsAb) that bind to transmembrane protein expressed at the BBB, such as the transferrin receptor (TfR), have shown enhanced brain exposure in rodents and non-human primate (NHP) due to receptor-mediated transcytosis. However, it remains unclear how preclinical findings translate to humans. Moreover, optimal TfR binding affinity remains a subject of debate. Model-informed drug discovery and development is a powerful approach that has been successfully used to support research and development. The goal of this analysis was to expand a published brain minimal physiologically based pharmacokinetic (mPBPK) model to investigate the optimal TfR binding affinity for maximal brain delivery in NHP and to facilitate prediction of the PK of anti-TfR bsAbs in humans from NHP data. Literature data for plasma, cerebrospinal fluid (CSF), and brain exposure after administration of non-TfR mAbs and monovalent bsAbs with respect to TfR in NHP were used to develop the TfR mPBPK model. Clinical validation using human PK data from plasma and CSF for the monovalent anti-TfR bsAb trontinemab demonstrated good predictive performance without major model recalibration. The availability of the TfR mPBPK model is envisaged to provide better understanding of the relationship between TfR binding affinity, dose, and brain exposure, which would lead to more robust selection of lead candidates and efficacious dosing regimens.

ARTICLE HISTORY
Received 17 February 2025
Revised 29 May 2025
Accepted 30 May 2025

KEYWORDS
TfR shuttling; mPBPK modeling; model-informed drug development (MIDD); brain delivery; pharmacokinetics (PK); Bispecific antibodies

Introduction

The development of monoclonal antibody (mAb) therapies for central nervous system (CNS) diseases, such as Alzheimer's disease (AD),[1] amyotrophic lateral sclerosis (ALS),[2] or Parkinson's disease[3] has been particularly challenging. A major obstacle for the development of antibody-based therapies for the treatment of CNS diseases is their poor brain penetration,[4] which is caused by the protective barriers surrounding the brain i.e., the blood–brain barrier (BBB). Yet, recent FDA approvals (e.g., lecanemab[5] and donanemab[6] for AD) have demonstrated the potential of mAbs in CNS diseases. High intravenous (IV) doses are, however, required to achieve efficacious exposure in the brain, which may not always be feasible due to safety concerns, infusion volumes, or cost of goods. Consequently, new methods for improving CNS-delivery of mAbs are critical for achieving desired efficacy, while also allowing for lower doses that may reduce safety concerns.

One of the possible strategies to enhance mAb brain penetration is the engineering of a bispecific antibody (bsAb), whereby one arm binds to the therapeutic target of interest, whilst the other arm targets a transmembrane protein expressed at the BBB to allow CNS uptake of macromolecules. This enables transport across the BBB via receptor-mediated transcytosis (RMT), followed by target engagement in the brain upon BBB transport. To date, the most-studied RMT systems at the BBB that have been investigated *in vivo* include the insulin receptor (IR),[7,8] the transferrin receptor (TfR),[9–12] and CD98 heavy chain (CD98hc).[10,12,13] Trontinemab is so far the most clinically advanced RMT system-targeting bsAb. It consists of a bispecific antibody composed of gantenerumab (a bivalent amyloid-beta (Aβ) mAb) Fab binding domains with an Fc C-terminal-conjugated human TfR binding domain. In non-human primate (NHP), trontinemab showed increased exposure in multiple brain regions, as measured by the area under the brain concentration *versus* time curve (AUC) by approximately 4–18-fold relative to gantenerumab.[9] Trontinemab was also predicted to yield enhanced brain exposure in humans,[14] and indeed has demonstrated the ability to clear amyloid more rapidly in people with AD at relatively low dose (3.6 mg/kg every 4 weeks),[15] in contrast to the currently approved anti-Aβ mAbs lecanemab (10 mg/kg every

CONTACT Morris Muliaditan m.muliaditan@lapp.nl Leiden Experts on Advanced Pharmacokinetics and Pharmacodynamics (LAP&P), Leiden, The Netherlands; Panteleimon D. Mavroudis panteleimon.mavroudis@sanofi.com Sanofi, Quantitative pharmacology-Pharmacometrics, 350 Water St., Cambridge, MA 02141, USA

Supplemental data for this article can be accessed online at https://doi.org/10.1080/19420862.2025.2515414.

2 weeks)[16] and donanemab (700 mg for the first three doses and 1400 mg thereafter, both given every 4 weeks).[17]

Model-based approaches have been applied to prospectively evaluate the impact of TfR binding affinity on TfR-mediated delivery and brain exposure.[18–22] However, none of those models were clinically validated. Furthermore, all published TfR-models were developed either using a full physiologically based pharmacokinetic (PBPK) approach[18,19] or empirically based frameworks.[20–22] There has been recently an increased interest in minimal-PBPK (mPBPK) models due to their relatively easy applicability whilst maintaining key mechanistic characteristics.[23,24] The mPBPK model has been developed by Bloomingdale et al.[25] and validated against the full PBPK model on which it was based,[18] focusing on assessing exposure of antibodies on CNS. Our analysis aimed to extend prior mPBPK efforts by incorporating TfR binding mechanisms to predict the plasma and CNS disposition of TfR bsAbs in NHP and humans. The model was extended based on the full PBPK model reported by Chang et al.[18] and used to evaluate the impact of TfR binding affinity on brain exposure in NHP and to predict the optimal binding affinity for future antibody therapeutics leveraging TfR-mediated drug delivery. Finally, despite limited data availability in humans, the mPBPK model was clinically validated against published exposure metrics of trontinemab in healthy participants.[26] While other TfR-targeting modalities such enzyme replacement therapy,[27] oligonucleotides,[28,29] or peptides[30,31] are being explored preclinically and/or clinically, this study focuses on monovalent TfR bsAbs.

Methods

Non-human primate and human pharmacokinetic data

Plasma, cerebrospinal fluid (CSF), and whole-brain homogenate concentration data for mAbs that do not bind to TfR (henceforth referred to as "non-TfR mAbs") or bsAbs that are monovalent with respect to TfR (henceforth referred to as "anti-TfR bsAbs") were collected from literature. Selected non-TfR mAbs were included based on brain/CSF pharmacokinetic (PK) data availability in the literature. In the published studies, concentration *versus* time profiles were derived following administration of single or repeated intravenous (IV) dosing. Mean values were digitized from literature using Digitizelt.[32] Individual PK profiles were available from one publication (Kariolis et al.).[33] Several studies evaluated antibody concentrations in various brain regions (e.g., cerebellum, cortex, or brainstem),[9,12,33,34] whilst others only reported whole-brain homogenate concentrations. In our analysis, brain region PK data were excluded unless whole-brain homogenate concentrations were not available. This was the case for brain data from two studies.[9,34] For simplicity, data from both the various brain regions and whole-brain homogenate were treated the same and are henceforth referred to as "brain" concentrations. All animals were perfused prior to preparation of the brain samples. An overview of the NHP studies that were included in this analysis is listed in Table 1. For the clinical validation, CSF concentrations and plasma exposure metrics following single ascending dose of 0.1, 0.4, 1.2, 3.6, and 7.2 mg/kg IV of trontinemab in healthy subjects were derived from ClinicalTrials.gov (NCT04023994).[26]

Development of the mPBPK model for anti-TfR bsAbs in non-human primates

Our TfR mPBPK model was developed based on combining the TfR binding components from Chang et al.[18] with the mPBPK model parameterization from Bloomingdale et al..[25] A schematic overview of the mPBPK TfR model is presented in Figure 1. All physiological parameterizations for antibody disposition in the Bloomingdale model (**Supplementary Materials, Table S1**) were retained except for the flow rate between the plasma and tissue compartment (Q_T). This parameter was originally based on the difference between lung (Q_L) and brain (Q_B) plasma flow. As the volume of the tissue compartment in the mPBPK was based upon the sum of the respective individual tissue compartments of a published full PBPK model for mAbs,[37] it was considered more appropriate to set Q_T to the volume-weighted average Q of all tissues (excluding brain) (**Supplementary Materials, Table S1**).

TfR association rate constant ($k_{on,TfR}$) and dissociation rate constant ($k_{off,TfR}$) were fixed to measured values, when available (**Supplementary Materials, Table S2**). In one study,[20] only $k_{on,TfR}$ and the dissociation constant for TfR ($K_{D,TfR}$) values were reported. In this case, $k_{off,TfR}$ was derived from the reported $k_{on,TfR}$ and $K_{D,TfR}$ values. For anti-TfR bsAbs for

Table 1. List of compounds included in the analysis.

Compound	Dose (mg/kg IV)	TfR K_D (nM)	Matrix	Reference
Control IgG	30	0	Plasma, CSF	Atwal 2011[35]
Anti-Tau-IgG	10	0	Plasma, Brain	Edavettal 2022[12]
TfR-K-mut	2, 10, 30	183	Plasma, CSF, Brain	Edavettal 2022[12]
TfR-J-wt	10	36	Plasma, Brain	Edavettal 2022[12]
TfR-J-mut	10	36	Plasma, Brain	Edavettal 2022[12]
Lu-AF82422	1, 3, 10, 30	0	Plasma, CSF	Fjord-Larsen 2021[36]
Gantenerumab	20	0	Plasma	Grimm 2023[9]
Trontinemab	10	249	Plasma, CSF, Brain	Grimm 2023[9]
Anti-TfR/BACE1	30	143, 343, 1650	Plasma	Kanodia 2016/ Chang 2022[18,20]
Control IgG	30	0	Plasma, Brain	Kariolis 2020[33]
ATV35.21.16:BACE1	30	1900	Plasma, Brain	Kariolis 2020[33]
Anti-BACE1	50	0	Plasma, CSF, Brain	Yadav 2017[34]
Control IgG	30	0	Plasma, Brain	Yu 2014[11]
Anti-TfR1-BACE1	30	37	Plasma, Brain	Yu 2014[11]
Anti-TfR2-BACE1	30	810	Plasma, Brain	Yu 2014[11]

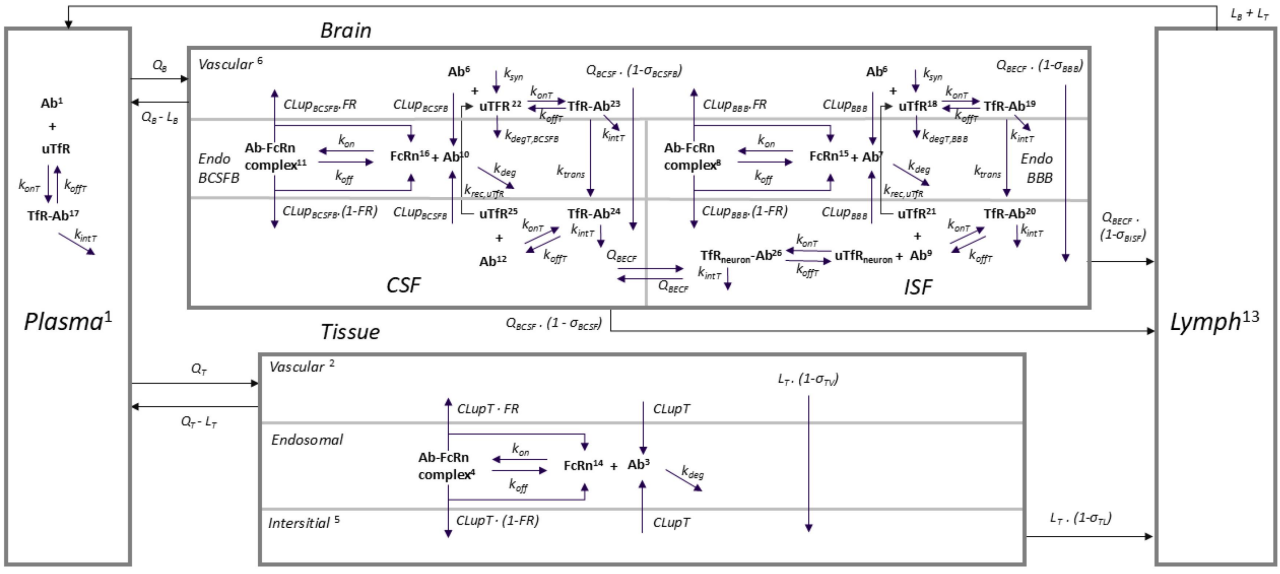

Figure 1. Schematic diagram of the mPBPK TfR model. Numbers represent the compartment number. Plasma flow between brain and non-brain tissues for unbound antibodies was implemented as Bloomingdale et al.,[25] while TfR-mediated disposition and transport were adapted from Chang et al.[18] hole-body (excluding brain) binding between anti-TfR bsAbs and TfR was described using an empirical TMDD mechanism in the plasma compartment. Unbound TfR in plasma was calculated as total plasma TfR (TfR_{pt}) minus the bsAb-TfR complex. In brain vascular, both antibodies can enter the brain ISF and CSF via the brain barriers BBB and BCSFB, respectively. Paracellular transport was assumed to occur through only the BCSFB for both non-TfR mAbs and anti-TfR bsAbs. Transcellular transport across the brain barriers via pinocytosis is described by nonspecific uptake clearance processes. Unbound antibodies in the endosome are eliminated through lysosomal degradation. Antibodies in brain endosomal spaces could also bind FcRn to form an antibody-FcRn complex, which either is taken up into the brain ISF and CSF or recycled back to the brain vasculature. In addition to pinocytosis, anti-TfR bsAbs can bind TfR to form a bsAb-TfR complex which undergoes TfR-mediated transcellular transport. The expression of TfR in the brain is included on the capillary endothelial cells (represented by uTfR on the BBB, referred to as $uTfR0_{BBB}$ in the main text), choroid plexus epithelial cells (represented by uTfR on the BCSFB, referred to as $uTfR0_{BCSFB}$ in the main text), and neurons in the brain ISF. Once in brain ISF and CSF, the bsAb-TfR complex could dissociate into unbound TfR and anti-TfR bsAb or be degraded. Unbound antibodies can distribute back to plasma via the glymphatic system while unbound TfR is recycled back to the brain vasculature. Unbound anti-TfR bsAbs in brain ISF could also bind to TfR on neurons and undergo elimination. Unbound TfR on neurons in brain ISF was calculated as total TfR on neurons (TfR_{totn}) minus the neuronal bsAb-TfR complex.

which only the $K_{D,TfR}$ values were reported,[11,33] $k_{off,TfR}$ was derived from the reported $K_{D,TfR}$ assuming a fixed $k_{on,TfR}$ of 0.5193 nM^{-1} h^{-1}, which represents the average $k_{on,TfR}$ values for the anti-TfR bsAbs in the dataset. $k_{on,TfR}$ was fixed to zero for the non-TfR mAbs. FcRn binding rate constants for the non-TfR mAbs and anti-TfR bsAbs were based on the Bloomingdale model[25] except for two compounds harboring YTE mutations (TfR-J-mut and TfR-K-mut)[12]. Since the authors did not report FcRn association/dissociation constants for these mutants, a 7-fold reduction in dissociation constant for FcRn ($K_{D,FcRn}$) was assumed based on reports from Borrok et al.[38] for motavizumab-YTE *versus* motavizumab. All non-TfR mAbs were assumed to display linear PK either in accordance with the study report[36] or based on the assumption that target binding was nearly saturated due to the relatively high doses (≥10 mg/kg) that were used in the respective studies. Binding to the therapeutic target of interest (e.g., BACE1) was therefore not included in the mPBPK model.

Characterization of TfR binding in plasma

Similar to Chang et al.,[18] our mPBPK model assumed that the plasma PK of anti-TfR bsAbs is mostly dominated by the high TfR levels in plasma. As such, the mPBPK model simplified the binding between drug and TfR to a single target-mediated drug disposition (TMDD) mechanism in the plasma compartment. More mechanistic approaches, such as inclusion of binding to TfR on red blood cells or in the tissue compartment of the mPBPK model, were not considered due to anticipated parameter unidentifiability issues caused by the lack of PK data in tissues other than brain for the selected anti-TfR bsAbs in the dataset we created for our analysis. Binding between anti-TfR bsAbs and TfR was included under the assumption that total (i.e., unbound + bound) TfR in plasma (TfR_{pt}) was constant. In our analysis, no distinction was made between soluble and membrane TfR in plasma to simplify the model structure. As such, estimated TfR_{pt} can be interpreted as the total (whole-body minus brain) concentration of TfR that is available for binding with the anti-TfR bsAbs at association rate constant $k_{on,TfR}$. Upon formation in plasma, the bsAb-TfR complex can either dissociate at rate constant $k_{off,TfR}$ or degrade at rate constant k_{int}, which was estimated from the PK data.

Characterization of TfR binding in brain

TfR binding was implemented in the following brain compartments in the mPBPK model: vascular, CSF and interstitial fluid (ISF). TfR concentrations on the luminal surface of the BBB ($uTFR0_{BBB}$) and blood–cerebrospinal fluid barrier (BCSFB) ($uTFR0_{BCSFB}$), i.e., brain vascular compartment in the mPBPK model, were estimated from the PK data and represent membrane TfR only. Elimination rate constants of TfR on the luminal surface of the BBB ($k_{deg,uTfRBBB}$) and BCSFB ($k_{deg,uTfRBCSFB}$) were initially fixed to the literature values used by Chang et al.,[18] i.e., 20 h^{-1} and 1.42 h^{-1}, respectively. Upon formation, the bsAb-TfR complex could be either eliminated at rate constant k_{int} or transported to the abluminal surface of the

BBB or BCSFB at first-order transcytosis rate constant (k_{trans}), which was fixed to $6\,h^{-1}$ as reported by Chang et al.[18] Once reaching the abluminal surface of the BBB (i.e., brain ISF compartment) or the BCSFB (i.e., CSF compartment), the bsAb-TfR complex could be either eliminated (at rate k_{int}) or dissociated (at rate $k_{off,TfR}$). The unbound TfR could then either associate with the unbound anti-TfR bsAb or, in contrast to the Chang model,[18] recycle back to the luminal surface of the BBB or BCSFB, which was assumed to occur at rate constant $k_{rec,uTfR}$. Unbound anti-TfR bsAbs in the brain ISF could also bind to TfR on neurons. Similar to TfR in plasma, total TfR on neurons in brain ISF (TfR_{totn}) was also assumed to be constant. TfR_{totn} was fixed to the value used by Chang et al.,[18] i.e., 559 nM.

Computation and model evaluation

The analysis was performed by means of non-linear mixed-effects modeling as implemented in the NONMEM software package (version 7.5.1, Icon Development Solutions, Ellicott City, Maryland USA)[39] using ADVAN8, in combination with PsN (version 5.3.0).[40,41] GFortran (version 9.4.0) was used as compiler. Parameters were estimated using the first-order conditional estimation method with interaction (FOCE-I). Diagnostic graphics, exploratory analyses, and post-processing of NONMEM output were performed using R (version 4.2.1, The R foundation for Statistical Computing),[42] and RStudio (version 2022.07.1–554, RStudio Inc, Boston, USA).[43] Simulation-based analyses were performed in R using the *mrgsolve* package.[44]

In general, the principle of parsimony was applied when comparing models during model development, meaning that the simplest model that described the data adequately was preferred. Standard Goodness-of-Fit (GoF) plots[45,46] were inspected visually to evaluate the model. A final model was also considered acceptable when the relative standard errors (RSE) of the structural parameter estimates are less than 50%. This would imply that the 95% confidence interval of the parameter estimate does not include zero, assuming normality.

Prediction of optimal TfR binding affinity in non-human primates

The final mPBPK model was subsequently used to investigate the relationship between $K_{D,TfR}$ (0, 30, 100, 300, 1000, 3000 nM) and brain exposure in NHP. Plasma and brain concentration *versus* time profiles up to 672 h (i.e., 28 days) post dose after single ascending IV doses (1, 3, 10, 30, 100 mg/kg) were simulated. Predicted brain exposure as measured by the area under the concentration curve until the last timepoint (i.e., $AUC_{0\text{-}672\,h}$) for the anti-TfR bsAbs (i.e., $K_{D,TfR} > 0$ nM) was subsequently compared against the predicted brain $AUC_{0\text{-}672\,h}$ for the non-TfR mAbs (i.e., $K_{D,TfR} = 0$ nM). AUC was calculated using the trapezoidal rule.

Translation of the mPBPK model from non-human primate to human

Clinical validation was performed against the following exposure metrics of trontinemab in healthy subjects[26:] the area under the plasma concentration *versus* time curve from 0 to 168 h post dose ($AUC_{0\text{-}168\,h}$), the area under the plasma concentration *versus* time curve from zero extrapolated to infinity ($AUC_{0\text{-}inf}$), concentration at the end of the infusion (C_{max}), and CSF concentrations at study day 3 and 5. Predicted $AUC_{0\text{-}inf}$ was approximated from $AUC_{0\text{-}56d}$. Prior to the human PK prediction, all physiological parameters (e.g., related to volume or flow) were replaced by the human equivalent from the Bloomingdale mPBPK model[25] (**Supplementary Materials, Table S1**). All TfR-related parameters were assumed to be the same in humans as in NHP except for $k_{on,TfR}$ and $k_{off,TfR}$, which were replaced to account for inter-species difference in TfR binding affinity ($K_{D,TfR}$ of 131 nM in human *versus* 249 nM in NHP).[9]

Results

mPBPK modeling and prediction of the optimal TfR binding affinity for brain exposure in NHP

The final NHP dataset contains 395 plasma concentrations, 81 CSF concentrations, and 102 brain concentrations from eight preclinical studies involving seven non-TfR mAbs and 10 anti-TfR bsAbs with $K_{D,TfR}$ ranging from 36 nM to 1900 nM. As the PK data spanned several orders of magnitude, drug concentrations were log-transformed to improve numerical stability.[47] Additive residual error on log scale was used, corresponding approximately to a proportional error on untransformed concentrations. Inter-individual variability was not evaluated as the dataset consisted mainly of mean values from various literature studies. PK data of both non-TfR mAbs and anti-TfR bsAbs were fitted simultaneously.

Initial evaluation of the published mPBPK model,[25] which has been validated against the full PBPK model on which it was based,[18] revealed systematic overprediction of the brain concentrations for the non-TfR mAbs in the dataset. A fixed correction factor (FAC_{BPRED}) was applied to account for the apparent bias in the original parameterization of the brain model. Further investigation by means of a local sensitivity analysis found that unrealistic alterations of physiological parameters would be required to achieve adequate brain predictions. Moreover, initial model development was performed assuming all measured plasma concentrations in the dataset corresponding to free drug. However, this approach led to poor performance, with all model variants assuming free drug concentration being statistically significantly inferior to the model that assumed total drug concentration in plasma (data not shown). Assuming plasma drug concentrations of anti-TfR bsAbs to be equal to total drug (i.e., free drug + drug-TfR complex) yielded the best overall performance. In contrast to Chang et al.,[18] $k_{deg,uTfRBCSFB}$ was fixed to $20\,h^{-1}$ (i.e., same as $k_{deg,uTfRBBB}$) to prevent total (i.e., sum of complex and unbound) TfR on BCSFB to decrease,

Table 2. Final parameter table for the NHP mPBPK TfR model.

Parameter [unit]	Estimate	RSE (%)	95% CI
TfR_{pt} [nM]	1672	38	(422, 2920)
$uTFR0_{BBB}$ [nM]	175	34	(59.1, 292)
$uTFR0_{BCSFB}$ [nM]	0.256	47	(0.0206, 0.492)
TfR_{totn} [nM][a]	559	FIXED	-
k_{trans} [h^{-1}][a]	6	FIXED	-
$k_{deg,uTfRBBB}$ [h^{-1}][a]	20	FIXED	-
$k_{deg,uTfRBCSFB}$ [h^{-1}][a]	20	FIXED	-
Fraction POP1	0.437	30	(0.180, 0.695)
k_{int} POP1 [h^{-1}]	0.0329	14	(0.0238, 0.0420)
k_{int} POP2 [h^{-1}]	0.0125	8.4	(0.0104, 0.0145)
$k_{rec,uTfR}$ [h^{-1}]	$=k_{int}$	FIXED	-
FAC_{BPRED} (factor)	0.05	FIXED	-
$FACQ_{BECF}$ (factor)	0.00814	29	(0.00347, 0.0128)
σ^2 add. Ln Plasma PK[b]	0.256	26	(0.124, 0.389)
σ^2 add. Ln CSF PK[b]	0.893	24	(0.469, 1.32)
σ^2 add. Ln Brain PK[b]	0.426	38	(0.106, 0.746)

Total plasma TfR concentration (TfRpt), membrane TfR concentration on the luminal surface of the BBB ($uTFR0_{BBB}$) and BCSFB ($uTFR0_{BCSFB}$), the total neuronal TfR concentrations in the brain ISF (TfR_{totn}), the transcytosis rate constant of bsAb-TfR complex at the BBB and BCSFB (k_{trans}), the degradation rate constant of unbound TfR at the BBB ($k_{deg,uTfRBBB}$) and BCSFB ($k_{deg,uTfRBCSFB}$), elimination rate constant for bsAb-TfR complex (k_{int}), subpopulation with "fast" k_{int} (POP1) and "slow" k_{int} (POP2), recycling rate constant for unbound TfR from brain ISF/CSF to brain vascular ($k_{rec,uTfR}$), correction factor for brain prediction (FAC_{BPRED}), correction factor to restrict the distribution of anti-TfR bsAbs from brain ISF to CSF ($FACQ_{BECF}$), additive residual error on natural log (Ln) concentrations (σ^2). Other model parameters (Supplementary Table S1) were obtained from the original brain mPBPK model described in Bloomingdale et al.[25]; [a]Fixed to values reported by Chang et al.[18]; [b]The additive error model was implemented as $y_{i,k} = PRED_{i,k} + \varepsilon$, where yi,k is the kth observation (log transformed) for the ith individual, PRED is the corresponding model predicted observation (log transformed) and ε represents the residual departure of the observed value from the individual predicted value, which was assumed to follow a normal distribution with mean zero and variance σ^2.

which was assumed to be biologically implausible. Estimated TfR levels in plasma and the luminal surface of the BBB and BCSFB in the final mPBPK TfR model were 1672 nM, 175 nM, and 0.256 nM, respectively. CSF concentrations of anti-TfR bsAbs were adequately predicted when the distribution of unbound bsAb from brain ISF to CSF was reduced. The final mPBPK TfR model also contained a mixture model for k_{int} to account for an apparent two subpopulations with "fast" and "slow" bsAb-TfR complex turnover in the dataset. Assuming $k_{rec,uTfR}$ to be equal to k_{int} led to the best performance in terms of model fit and stability. Key parameters in the NHP mPBPK TfR model are shown in Table 2.

As shown by the GoF plots and fit plots, the final mPBPK TfR model was able to describe the PK data well for both the non-TfR mAbs and anti-TfR bsAbs (Figures 2 and 3, respectively). Plasma, CSF, and/or brain concentrations were captured by the mPBPK TfR model in most of the studies/compounds but not for all. Plasma concentrations of the non-TfR mAb from Kariolis et al.[33] indicated faster than expected elimination for a typical mAb (Figure 2). In addition, CSF concentrations of the non-TfR mAbs from Atwal 2011 and Yadav 2017 appeared to be lower than the predicted CSF levels for a typical mAb in the current mPBPK model. Brain concentrations were underpredicted for the anti-TfR bsAbs in the high binding affinity range: TfR-J-wt and TfR-J-mut (Edavettal 2022, $K_{D,TfR}$ = 36 nM), and anti-TfR-1-BACE1 (Yu 2014, $K_{D,TfR}$ = 37 nM) (Figure 3). Simulations using the mPBPK model predicted that optimal brain AUC in NHP can be achieved with $K_{D,TfR}$ in the range of 800–3000 nM (Figure 4). Simulated PK profiles at varying TfR binding affinity are shown in **Supplementary Materials** (**Figure S2**).

Translation of trontinemab pharmacokinetics from non-human primate to human

The NHP mPBPK model was subsequently scaled to human by replacing all physiological parameters (i.e., flows and volumes) to the human equivalent values as reported by Bloomingdale et al.[25] TfR-related parameter values were assumed to be the same between NHP and human except for $K_{D,TfR}$ (131 nM in human *versus* 249 nM in NHP).[9] Initial predictions showed a reasonable predicting capacity of the model without changing any additional parameters (Figures 5a,c). Performance for plasma exposure was improved by allometric scaling of a single parameter (k_{int}) that we expect to be slightly different between species (Figures 5b,c). The allometrically scaled trontinemab k_{int} for a 70 kg human from the estimated 6.2 kg NHP value of 0.0329 h^{-1} using a standard exponent of −0.25[50] was 0.0179 h^{-1}. Further improvement of performance for CSF concentrations was achieved by recalibrating $uTFR0_{BCSFB}$ to be approximately 3-fold higher in humans compared to NHP (Figures 5b,c).

Discussion

Published TfR models have so far utilized either a full PBPK or empirical approach.[9,18–21] Whilst full PBPK models have become the gold standard for investigating tissue dispositions of mAbs, their use could also be quite complex especially for new entities and computationally expensive. On the other hand, an empirical compartment model may not be suitable when there is a need for prospective predictions involving hypothetical scenarios in the absence of *in vivo* data or for gaining quantitative insights about mechanism of disposition kinetics of new molecular entities. Consequently, an

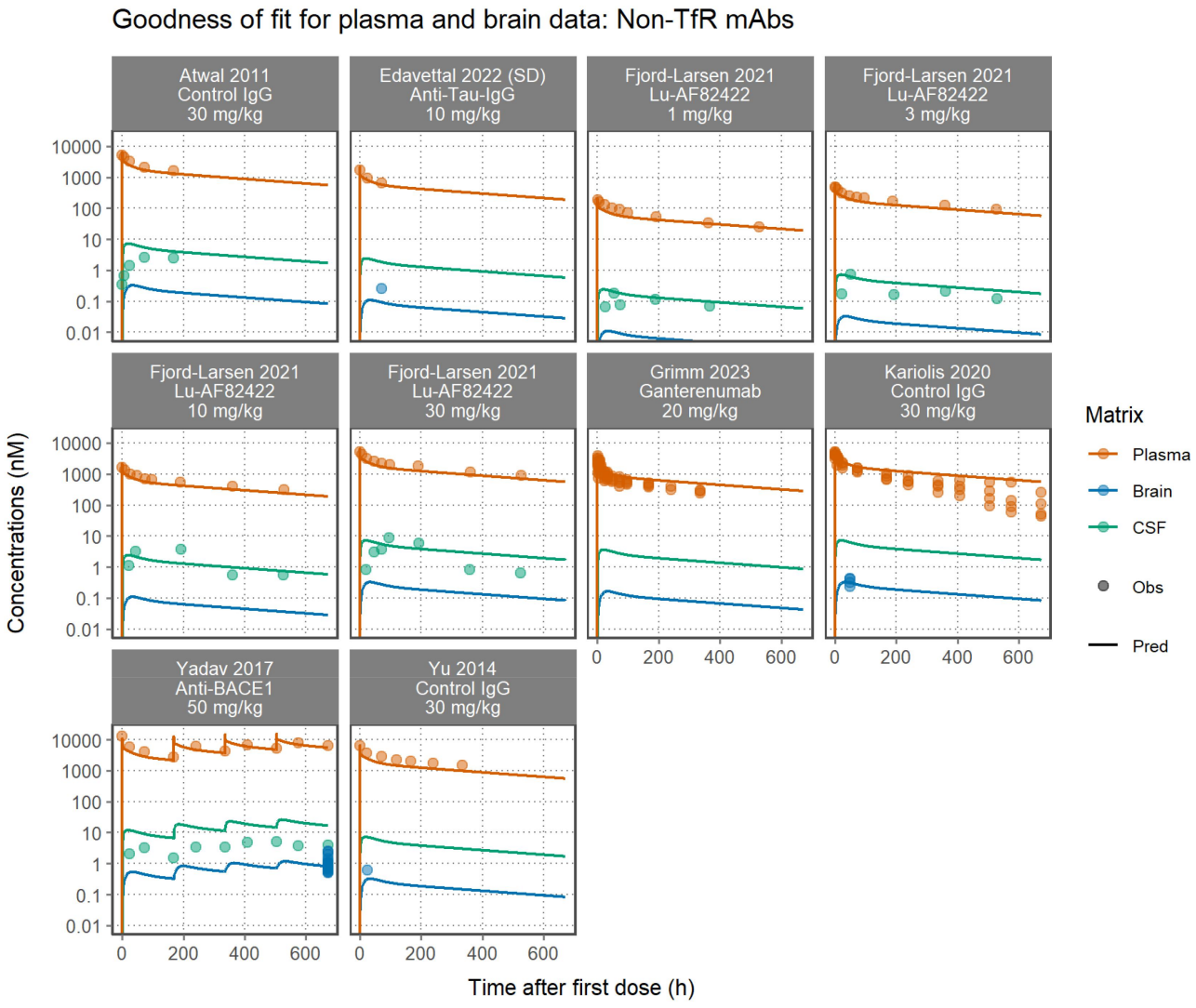

Figure 2. Model fit for PK profiles of non-TfR mAbs in NHP. Predictions (solid lines) and observations (circles) are shown for plasma, brain and CSF. In most studies, NHP received a single dose IV of the non-TfR mAb, except for Yadav 2017 in which NHP received four weekly infusions of the non-TfR mAb. Data source, compound name (or the target protein), and dose are shown in the panel labels.

intermediate mPBPK model for TfR antibody therapeutics is presented here which could enable more mechanistic predictions of brain exposure than compartment models, whilst still sufficiently accounting for relevant physiological processes[23] and remaining parsimonious.

NHP is often the only species in which the (humanized) antibody can cross react with the target of interest. Although tissue PK is rarely collected in NHP, it is therefore relatively the most relevant species for nonclinical PK or pharmacokinetics-pharmacodynamics (PK/PD) assessment of antibodies.[48,49] As such, we did not consider modeling PK data from other species (i.e., mouse and rat) in contrast to other published PBPK works.[18,19] However, our model can be easily scaled to rodents when needed by simply replacing the underlying physiological parameters (i.e., volumes and flow rates) with rodent values,[25] together with re-estimation of the TfR-related parameters. It should be noted that it is currently unclear how the PK of TfR bsAbs scale across preclinical species and humans. For instance, the translation of the rodent model to the monkey PBPK model in the Chang et al. analysis required additional estimation of both k_{int} and TfR levels in plasma and BBB.[18] Our analysis found that scaling of k_{int} in the NHP mPBPK model was indeed required to better predict trontinemab PK in healthy subjects (Figure 5). This finding is consistent with the expectation based on allometric principles that physiological turnover rate constants decrease with increasing body weight across species.[50] Our clinical validation moreover revealed that recalibration of TfR expression on BCSFB (i.e., $uTFR0_{BCSFB}$) in humans was needed to improve the prediction accuracy for CSF concentrations. Chang et al. identified a higher TfR levels in plasma and BBB in NHP as compared to rodents.[18] Whilst more translational work is needed, these results suggested that TfR levels and turnover in plasma and brain may vary across species. Our analysis showed that adequate human PK predictions for anti-TfR bsAbs can be achieved using NHP as the primary species. Nonetheless, rodent models remain valuable for supporting target identification and validation (often conducted in mouse efficacy studies), selecting drug candidates for NHP studies, and

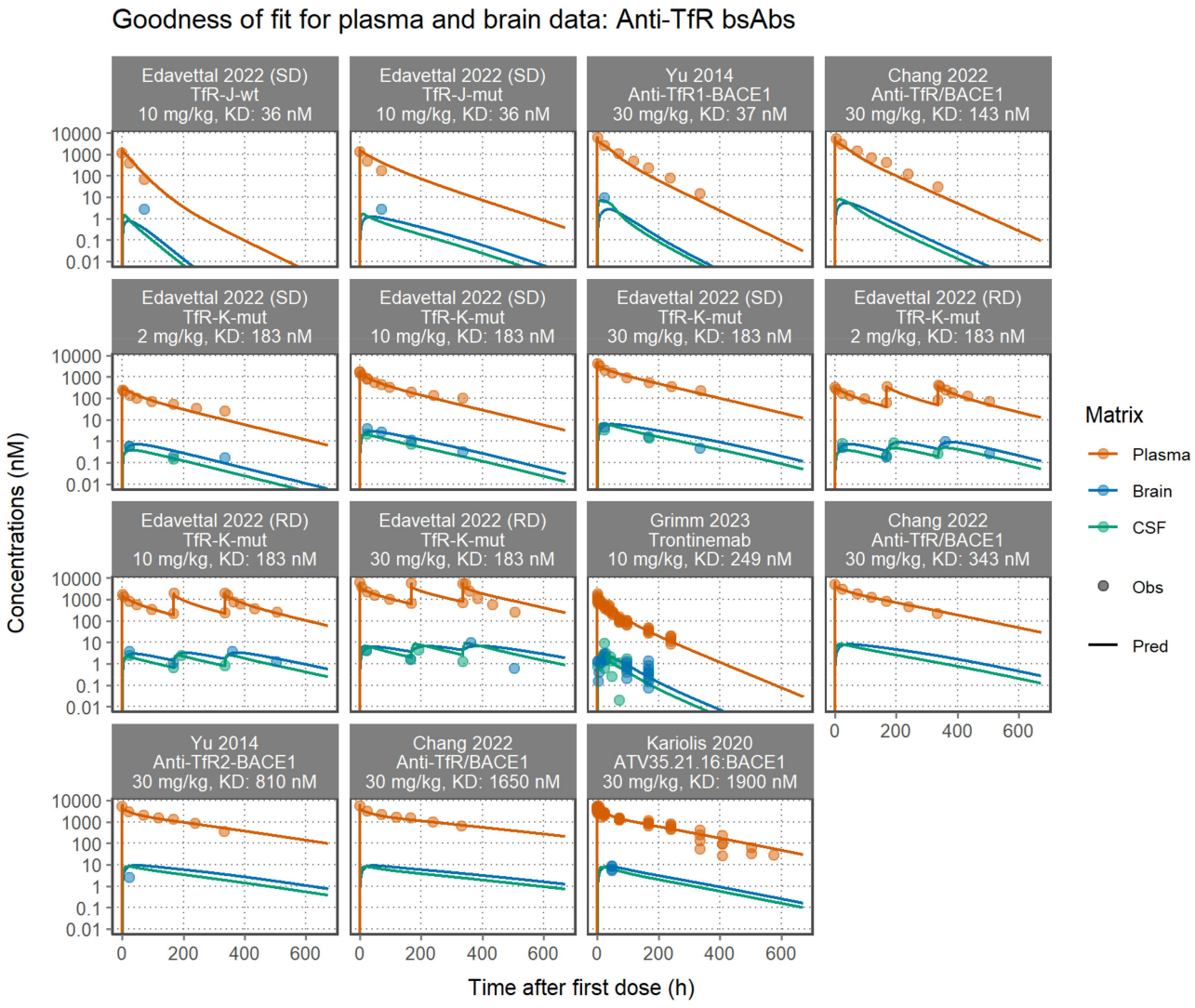

Figure 3. Model fit for PK profiles of anti-TfR bsAbs in NHP. Predictions (solid lines) and observations (circles) are shown for plasma, brain and CSF. In Edavettal 2022 study, NHP received either single ascending (SD) or multiple ascending (RD) doses, given every three weeks. NHP in other studies received a single IV dose of the anti-TfR bsAb. Data source, compound name (or the target proteins), dose, and $K_{D,TfR}$ are shown in the panel labels.

informing early human dose projections when NHP data is unavailable. Whilst beyond the scope of this analysis, additional investigations focusing on the evaluation of the predictive performance of the mPBPK model trained with additional animal models (e.g., human TfR knock-in mice[11,26,33] for anti-TfR bsAbs PK in human could be of interest in the future.

To our best knowledge, our mPBPK TfR model was developed based on the most comprehensive NHP brain/CSF PK dataset to date compared to published PBPK models developed by Chang et al.[18] or Sato et al.[19] The mPBPK model was validated against NHP brain/CSF data from 10 unique anti-TfR bsAbs *versus* six in Chang et al.[18] and five in Sato et al.[19] Moreover, we also included NHP brain/CSF PK data from more non-TfR mAbs (six *versus* one in Chang et al.[18] and two in Sato et al..[19] In contrast to both PBPK works, we chose to focus on developing a mPBPK framework specifically for monovalent bsAbs with respect to TfR. Other modalities (i.e., the recombination fusion protein) JR-141 as included in Sato et al.[19] were therefore excluded. In contrast to both PBPK analyses, we also chose to exclude the bivalent TfR mAb (i.e., hTfRmAb51) from this analysis due to considerable differences in transport mechanisms with monovalent anti-TfR bsAbs which may require additional parameterization in the framework mPBPK model. While a monovalent TfR binding facilitates transcellular transport, bivalent TfR binding has namely been associated with impaired brain transport due to lysosomal sorting and downregulation of cell surface TfR[52] (although the degree of impairment is likely dependent on binding affinity). Development of a framework mPBPK model that can describe drug disposition differences between TfR modalities or binding mode (i.e., monovalent *versus* bivalent) was beyond the scope of this work but may be considered in the future.

We found that the original mPBPK model[25] overpredicted the brain concentrations of the non-TfR mAbs in our NHP dataset. The original mPBPK model was calibrated such that predicted brain concentrations for non-TfR mAbs were approximately the same as in CSF. Yet, CSF is not a surrogate of the brain ISF compartment, as both are

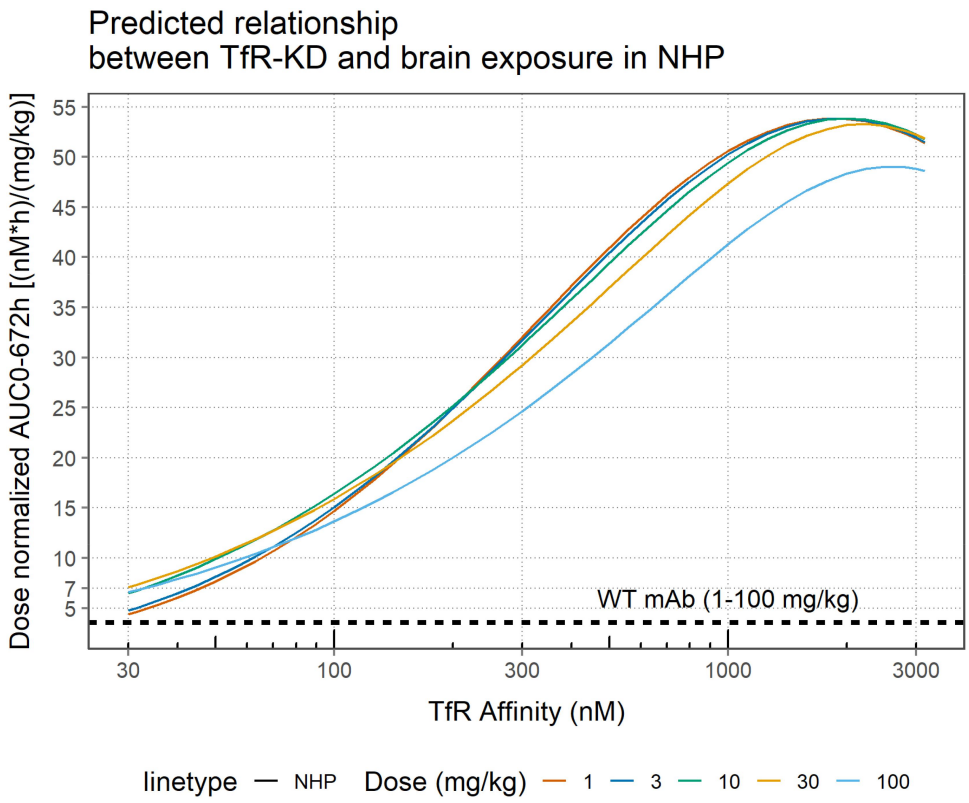

Figure 4. Predicted relationship between TfR binding affinity and dose-normalized brain $AUC_{0\text{-}672\,h}$ in NHP. In the simulations, NHP received single ascending doses (1–100 mg/kg) administered as a single bolus intravenous infusion. The horizontal dashed line represents the predicted dose-normalized brain $AUC_{0\text{-}672\,h}$ for a non-TfR mAb (i.e., $K_{D,TfR} = 0$ nM).

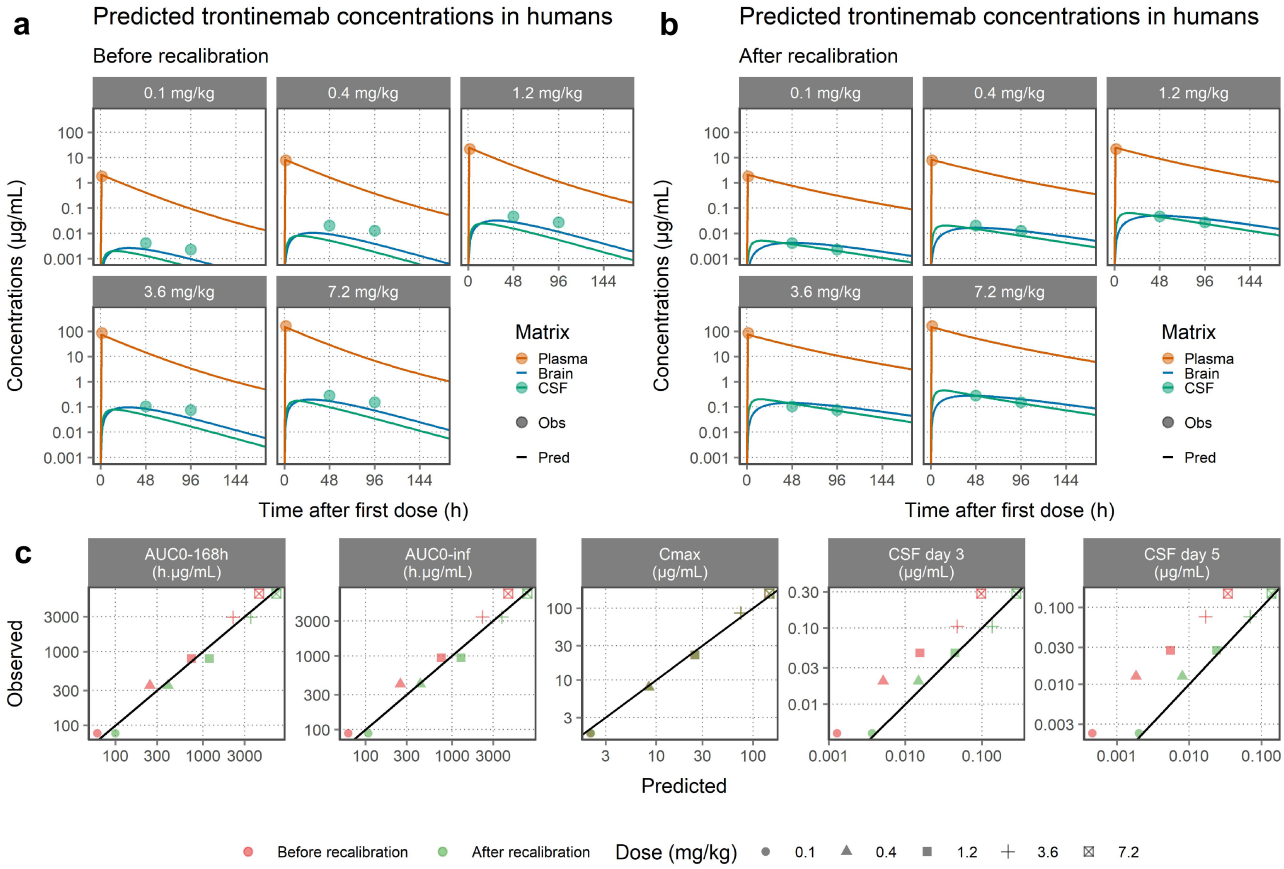

Figure 5. Predictions of trontinemab concentration in plasma, brain and CSF *versus* time profiles in healthy subjects before (a) and after model recalibration (b). Healthy subjects received single ascending doses of trontinemab (0.1–7.2 mg/kg) administered as an intravenous infusion. Predictions are shown as solid lines while observations are represented by the circles. (c) Comparison of predicted *versus* observed exposure metrics in plasma and CSF before (red symbols) and after recalibration (green symbols). Symbol shapes represent the trontinemab dose. Solid line: line of identity.

separated by two distinct barriers (BCSFB and BBB, respectively) with different properties. The assumption of lower brain exposure (relative to CSF) for non-TfR mAbs in the current mPBPK model seems to be more consistent with the underlying physiology[4] and our NHP dataset.[11,12,33,34] Subsequent sensitivity analysis revealed that achieving adequate brain predictions would require unrealistic alterations of physiological parameters (e.g., brain volumes or brain uptake clearance rate). Finally, as these changes were deemed biologically implausible, a fixed correction factor (FAC_{BPRED}) was considered as an empirical approach to address the apparent bias in the original brain model parameterization. It should be noted that the measurement of brain homogenate is difficult to interpret, e.g., incomplete perfusion could lead to artificially several fold higher exposures of antibody in brain homogenate.[53] Whilst assumed negligible in our analysis, contamination by residual blood is therefore a major potential source of variability for observed brain concentrations that could not be ruled out. In addition, in our analysis, plasma drug concentrations of anti-TfR bsAbs had to be assumed to be equal to total drug in order to achieve adequate fit of the NHP PK data. All attempts to incorporate the free drug assumption led to statistically inferior models. Furthermore, extension of the mPBPK model to include differentiation between soluble and membrane-bound TfR (sTfR and mTfR, respectively) are expected to cause identifiability issues in the absence of TfR measurements. Further investigation is clearly warranted.

During our model development, we found that transport of anti-TfR bsAbs from the brain ISF to CSF had to be significantly reduced to explain the lower gain in CSF concentrations as compared to brain. This finding is consistent with the hypothesis of transferal across the BBB being the dominant transport mechanism into the CNS for anti-TfR bsAbs, whilst non-TfR mAbs enter the CNS via the CSF.[9,33,54] Furthermore, the inclusion of a mixture model identified two populations with "fast" and "slow" k_{int} values ($0.0329\ h^{-1}$ and $0.0125\ h^{-1}$, respectively or approximately two-fold difference), which were not correlated to $K_{D,TfR}$ or data source. Mixture models have been commonly used to describe latent multimodal distributions of drug elimination[55,56] and are especially useful when the source of variability is unknown (e.g., genotype). However, more investigation is warranted to better understand whether the identified variability is simply random or could be explained by compound/study-specific properties. The predicted optimal TfR binding affinity in NHP based on our mPBPK model was between 800 and 3000 nM. This range is similar to model-based predictions from Sato et al.[19] (100–-10000 nM in NHP) and slightly higher than predicted by Chang et al.[18] (100–750 nM in rats). Kanodia et al.[20] predicted an optimal binding affinity of 100–300 nM in humans based on optimizing average and maximal peak Aβ inhibition. Sato et al.[19] predicted a comparable optimal binding affinity between NHP and human (i.e., 100–10000 nM) based on total brain exposure. It should be noted that the exact optimal binding affinity for anti-TfR bsAbs is expected to vary from species to species (e.g., between rodents and NHP), as well as from target to target.[11]

We envision that more validation of the translational mPBPK model is needed (particularly in humans) before predictions of the optimal binding affinity in humans can be performed with reasonable robustness. Overall, whilst there is some inconsistency between literature values, all modeling works thus far are consistent in postulating the optimal TfR binding affinity to be in the range of ≥100 nM. It should be noted that brain concentrations were limited to a single timepoint for most of the anti-TfR bsAbs, which especially hampered the assessment of the predictive performance of the mPBPK model for brain concentration profiles at the high TfR binding affinity range (e.g., 36–37 nM). Longitudinal brain PK data were available from two studies only, with TfR binding affinity range limited to 183–249.[9,12] The inclusion of brain concentrations collected at multiple time points would greatly benefit future validation of this mPBPK model, especially for anti-TfR bsAbs with high binding affinity range, for which brain concentrations were underpredicted by the current mPBPK model.

Our mPBPK analysis has several limitations. PK data of anti-TfR bsAbs in the training dataset was restricted to mainly single, relatively high-dose range (10–30 mg/kg) with low dose (2 mg/kg) PK data only available from Edavettal 2022.[12] More investigation with additional data is warranted to ascertain whether the model could predict PK at both low and high doses, as well as following multiple ascending doses. Moreover, the current mPBPK model is not yet ready to support PK analysis of drugs that are directly administered into the CNS (e.g., via intrathecal or intracerebroventricular injection) as the model has been trained using IV PK data only. Future refinement of the model could, however, benefit from PK data following intrathecal or intracerebroventricular injection, as it may help reveal some of the processes in the brain in more detail (e.g., drug exchange between CSF and brain ISF). Our mPBPK analysis also focuses on whole-brain homogenate concentrations, which may not be representative for concentration in the target brain region. Interestingly, trontinemab regional exposures in NHP were found to be more homogenously distributed compared to gantenerumab.[9] Whilst further evidence is needed, we postulate as such that anti-TfR bsAbs may offer the advantage of a more homogenous penetration of the brain tissue in comparison to non-TfR mAbs. Nevertheless, future refinements could include partitioning of the brain compartment in the mPBPK model into subregion(s) of interests[57] to support the development of anti-TfR bsAbs targeting specific region of the brain.

Another important point to consider is that current model predicts that the brain ISF concentration is dependent on TfR binding. In particular, predicted ISF concentration for the anti-TfR bsAbs in both NHP and human is higher than non-binder/wild type (**Supplementary Results, Figure S3**). Sensitivity analysis showed that levels of anti-TfR bsAbs in brain ISF are sensitive to $uTFR0_{BBB}$, k_{trans} or TfR_{totn} (**Supplementary Results, Figure S4**). Lower brain ISF levels can be achieved by changing these parameters but simultaneously led to worse performance for brain homogenate. As further validation was hampered by the lack of experimental brain ISF data, the current mPBPK model cannot be used to simulate concentrations of anti-TfR bsAbs in brain ISF. Predicted concentrations in brain homogenate or CSF can be used instead as surrogate for drug exposure in the brain.

Sensitivity analysis of the model also revealed unexpected behavior for the anti-TfR bsAbs shortly after dosing (i.e., approximately 24-h post dose). In this time frame, concentrations representing total drug were found to increase with decreasing $K_{D,TfR}$ relative to predicted concentrations of a non-TfR mAb (**Supplementary Results, Figure S5**). Whilst total drug concentration of any anti-TfR bsAbs is not expected to exceed the drug concentrations of a non-TfR mAb at any given timepoint in plasma, we expect the impact of this behavior for decision-making to be minimal as it is restricted to just 24-h post dose, which is negligible when compared to a typical dosing interval for antibody therapeutics (i.e., weeks). Finally, clinical validation of the mPBPK model was based on human PK data from a single compound (trontinemab). Whilst initial analysis showed promising results, more clinical validation is warranted. To our knowledge, human PK data in public domain is available for only two TfR antibodies, namely trontinemab[14] and PPMX-T003.[58] Human PK data from PPMX-T003 was considered too limited for model validation as plasma concentrations were available for up to 48-h post dose only, without disclosure of any brain or CSF data.

In summary, a mPBPK TfR model was developed based on NHP data, which adequately predicted the PK of an anti-TfR bsAb (trontinemab) in humans after inter-species scaling of relevant parameters. The availability of the mPBPK TfR model is envisaged to provide better understanding of the impact of TfR binding affinity on dose and brain exposure, which would lead to more robust selection of lead candidates and efficacious dosing regimens for clinical development.

Acknowledgments

The authors would like to thank Martijn van Noort for reviewing the mPBPK model. We also would like to thank Majid Vakilynejad for his valuable comments on the manuscript.

Disclosure statement

The authors Lindsay B. Avery, Wei Sun, Timothy R. Hammond, Siak-Leng Choi, Nikhil Pillai, Nina C. Leksa, and Panteleimon D. Mavroudis are employees of Sanofi and may hold stock and/or stock options. Morris Muliaditan, Tamara van Steeg, and Diana Hijdra are employees of LAP&P and consultants for Sanofi.

Funding

This study was funded by Sanofi.

ORCID

Tamara J. van Steeg http://orcid.org/0000-0003-1387-1369
Nina C. Leksa http://orcid.org/0000-0003-0331-4323
Panteleimon D. Mavroudis http://orcid.org/0000-0002-0512-4147

References

1. Cummings J, Osse AML, Cammann D, Powell J, Chen J. Anti-amyloid monoclonal antibodies for the treatment of Alzheimer's disease. BioDrugs. 2024;38(1):5–22. doi: 10.1007/s40259-023-00633-2.
2. Genge A, van den Berg Lh, Frick G, Han S, Abikoff C, Simmons A, Lin Q, Patra K, Kupperman E, Berry JD, et al. Efficacy and safety of Ravulizumab, a complement C5 inhibitor, in adults with amyotrophic lateral sclerosis: a randomized clinical trial. JAMA Neurol. 2023;80(10):1089–1097. doi: 10.1001/jamaneurol.2023.2851.
3. Kharel S, Ojha R. Future of monoclonal antibody therapy in Parkinson's disease. Ann Neurosci. 2023;30(1):8–10. doi: 10.1177/09727531221136349.
4. Pardridge WM. Receptor-mediated drug delivery of bispecific therapeutic antibodies through the blood-brain barrier. Front Drug Deliv. 2023;3:1227816. doi: 10.3389/fddev.2023.1227816.
5. Harris E. Alzheimer drug lecanemab gains traditional FDA approval. JAMA. 2023;330(6):495. doi: 10.1001/jama.2023.12548.
6. Kang C. Donanemab: first approval. Drugs. 2024;84(10):1313–1318. doi: 10.1007/s40265-024-02087-4.
7. Pardridge WM, Kang YS, Buciak JL, Yang J. Human insulin receptor monoclonal antibody undergoes high affinity binding to human brain capillaries in vitro and rapid transcytosis through the blood-brain barrier in vivo in the primate. Pharm Res. 1995;12(6):807–816. doi: 10.1023/A:1016244500596.
8. Boado RJ, Pardridge WM. Brain and organ uptake in the rhesus monkey in vivo of recombinant iduronidase compared to an insulin receptor antibody-iduronidase fusion protein. Mol Pharm. 2017;14(4):1271–1277. doi: 10.1021/acs.molpharmaceut.6b01166.
9. Grimm HP, Schumacher V, Schäfer M, Imhof-Jung S, Freskgård P-O, Brady K, Hofmann C, Rüger P, Schlothauer T, Göpfert U, et al. Delivery of the Brainshuttle™ amyloid-beta antibody fusion trontinemab to non-human primate brain and projected efficacious dose regimens in humans. mAbs 2023; Mabs-austin. 2023;15(1):2261509. doi: 10.1080/19420862.2023.2261509.
10. Pornnoppadol G, Bond LG, Lucas MJ, Zupancic JM, Kuo Y-H, Zhang B, Greineder CF, Tessier PM. Bispecific antibody shuttles targeting CD98hc mediate efficient and long-lived brain delivery of IgGs. Cell Chem Biol. 2024;31(2):361–372.e8. doi: 10.1016/j.chembiol.2023.09.008.
11. Yu YJ, Atwal JK, Zhang Y, Tong RK, Wildsmith KR, Tan C, Bien-Ly N, Hersom M, Maloney JA, Meilandt WJ, et al. Therapeutic bispecific antibodies cross the blood-brain barrier in nonhuman primates. Sci Transl Med [internet]. 2014 [cited 2024 June 24]. 6. 261). d oi: https://www.science.org/d oi/10.1126/scitranslmed.3009835.
12. Edavettal S, Cejudo-Martin P, Dasgupta B, Yang D, Buschman MD, Domingo D, Van Kolen K, Jaiprasat P, Gordon R, Schutsky K, et al. Enhanced delivery of antibodies across the blood-brain barrier via TEMs with inherent receptor-mediated phagocytosis. Med. 2022;3(12):860–882.e15. doi: 10.1016/j.medj.2022.09.007.
13. Chew KS, Wells RC, Moshkforoush A, Chan D, Lechtenberg KJ, Tran HL, Chow J, Kim DJ, Robles-Colmenares Y, Srivastava DB, et al. CD98hc is a target for brain delivery of biotherapeutics. Nat Commun. 2023;14(1):5053. doi: 10.1038/s41467-023-40681-4.
14. Abrantes JA. PK/PD modeling framework to inform the clinical development of RG6102, an amyloid-targeting investigational drug with enhanced brain penetration properties [Internet]. 2019 [cited 2024 June 24]. https://medically.roche.com/global/en/medical-material/CTAD-2021-presentation-abrantes-pk-pd-modeling-framework-to-inform-the-clinical-development-of-RG6102-pdf.html.
15. Bonni A. Roche neurology update. [Internet]. 2024 [cited 2024 Nov 26]. https://assets.roche.com/f/176343/x/bdd463f4af/roche-neurology-ir-event-2024.pdf.
16. van Dyck Ch, Swanson CJ, Aisen P, Bateman RJ, Chen C, Gee M, Kanekiyo M, Li D, Reyderman L, Cohen S, et al. Lecanemab in early Alzheimer's disease. N Engl J Med. 2023;388(1):9–21. doi: 10.1056/NEJMoa2212948.
17. Sims JR, Zimmer JA, Evans CD, Lu M, Ardayfio P, Sparks J, Wessels AM, Shcherbinin S, Wang H, Monkul Nery ES, et al.

Donanemab in early symptomatic Alzheimer disease: the TRAILBLAZER-ALZ 2 randomized clinical trial. JAMA. 2023;330(6):512–527. doi: 10.1001/jama.2023.13239.
18. Chang H-Y, Wu S, Chowdhury EA, Shah DK. Towards a translational physiologically-based pharmacokinetic (PBPK) model for receptor-mediated transcytosis of anti-transferrin receptor monoclonal antibodies in the central nervous system. J Pharmacokinet Pharmacodyn. 2022;49(3):337–362. doi: 10.1007/s10928-021-09800-w.
19. Sato S, Liu S, Goto A, Yoneyama T, Okita K, Yamamoto S, Hirabayashi H, Iwasaki S, Kusuhara H. Advanced translational PBPK model for transferrin receptor-mediated drug delivery to the brain. J Control Release. 2023;357:379–393. doi: 10.1016/j.jconrel.2023.04.012.
20. Kanodia J, Gadkar K, Bumbaca D, Zhang Y, Tong R, Luk W, Hoyte K, Lu Y, Wildsmith K, Couch J, et al. Prospective design of anti-transferrin receptor bispecific antibodies for optimal delivery into the human brain. CPT Pharmacom & Syst Pharma. 2016;5:283–291. doi: 10.1002/psp4.12081.
21. Gadkar K, Yadav DB, Zuchero JY, Couch JA, Kanodia J, Kenrick MK, Atwal JK, Dennis MS, Prabhu S, Watts RJ, et al. Mathematical PKPD and safety model of bispecific TfR/BACE1 antibodies for the optimization of antibody uptake in brain. Eur J Pharm Biopharm. 2016;101:53–61. doi: 10.1016/j.ejpb.2016.01.009.
22. Pardridge WM, Chou T. Mathematical models of blood-brain barrier transport of monoclonal antibodies targeting the transferrin receptor and the insulin receptor. Pharmaceuticals (Basel). 2021;14(6):535. doi: 10.3390/ph14060535.
23. Cao Y, Balthasar JP, Jusko WJ. Second-generation minimal physiologically-based pharmacokinetic model for monoclonal antibodies. J Pharmacokinet Pharmacodyn. 2013;40(5):597–607. doi: 10.1007/s10928-013-9332-2.
24. Cao Y, Jusko WJ. Applications of minimal physiologically-based pharmacokinetic models. J Pharmacokinet Pharmacodyn. 2012;39(6):711–723. doi: 10.1007/s10928-012-9280-2.
25. Bloomingdale P, Bakshi S, Maass C, van Maanen E, Pichardo-Almarza C, Yadav DB, van der Graaf P, Mehrotra N. Minimal brain PBPK model to support the preclinical and clinical development of antibody therapeutics for CNS diseases. J Pharmacokinet Pharmacodyn. 2021;48(6):861–871. doi: 10.1007/s10928-021-09776-7.
26. Roche H-L. A single ascending dose study to investigate the safety, tolerability, immunogenicity and pharmacokinetics of intravenously administered RO7126209 in healthy participants. https://clinicaltrials.gov/study/NCT04023994.
27. Kida S, Koshimura Y, Yoden E, Yoshioka A, Morimoto H, Imakiire A, Tanaka N, Tanaka S, Mori A, Ito J, et al. Enzyme replacement with transferrin receptor-targeted α-L-iduronidase rescues brain pathology in mucopolysaccharidosis I mice. Mol Ther - Methods Clin Devel. 2023;29:439–449. doi: 10.1016/j.omtm.2023.05.010.
28. Barker SJ, Thayer MB, Kim C, Tatarakis D, Simon MJ, Dial R, Nilewski L, Wells RC, Zhou Y, Afetian M, et al. Targeting the transferrin receptor to transport antisense oligonucleotides across the mammalian blood-brain barrier. Sci Transl Med. 2024;16(760):eadi2245. doi: 10.1126/scitranslmed.adi2245.
29. Hammond SM, Abendroth F, Goli L, Stoodley J, Burrell M, Thom G, Gurrell I, Ahlskog N, Gait MJ, Wood MJ, et al. Antibody-oligonucleotide conjugate achieves CNS delivery in animal models for spinal muscular atrophy. JCI Insight. 2022;7(24):e154142. doi: 10.1172/jci.insight.154142.
30. Crook ZR, Girard E, Sevilla GP, Merrill M, Friend D, Rupert PB, Pakiam F, Nguyen E, Yin C, Ruff RO, et al. A TfR-Binding cystine-dense peptide promotes blood-brain barrier penetration of bioactive molecules. J Mol Biol. 2020;432(14):3989–4009. doi: 10.1016/j.jmb.2020.04.002.
31. McQuaid C, Halsey A, Dubois M, Romero I, Male D, Deli MA. Comparison of polypeptides that bind the transferrin receptor for targeting gold nanocarriers. PLOS ONE. 2021;16(6):e0252341. doi: 10.1371/journal.pone.0252341.
32. Bormann I. DigitizeIt (version 2.1.2): Bormisoft. 2020. http://www.digitizeit.xyz.
33. Kariolis MS, Wells RC, Getz JA, Kwan W, Mahon CS, Tong R, Kim DJ, Srivastava A, Bedard C, Henne KR, et al. Brain delivery of therapeutic proteins using an Fc fragment blood-brain barrier transport vehicle in mice and monkeys. Sci Transl Med. 2020;12(545):eaay1359. doi: 10.1126/scitranslmed.aay1359.
34. Yadav DB, Maloney JA, Wildsmith KR, Fuji RN, Meilandt WJ, Solanoy H, Lu Y, Peng K, Wilson B, Chan P, et al. Widespread brain distribution and activity following i.c.v. infusion of anti-β-secretase (BACE1) in nonhuman primates. Br J Pharmacol. 2017;174(22):4173–4185. doi: 10.1111/bph.14021.
35. Atwal JK, Chen Y, Chiu C, Mortensen DL, Meilandt WJ, Liu Y, Heise CE, Hoyte K, Luk W, Lu Y, et al. A therapeutic antibody targeting BACE1 inhibits amyloid-β production in vivo. Sci Transl Med [internet]. 2011 [cited 2024 June 24]. 3. d oi: https://www.science.org/d oi/10.1126/scitranslmed.3002254.
36. Fjord-Larsen L, Thougaard A, Wegener KM, Christiansen J, Larsen F, Schrøder-Hansen LM, Kaarde M, Ditlevsen DK. Nonclinical safety evaluation, pharmacokinetics, and target engagement of Lu AF82422, a monoclonal IgG1 antibody against alpha-synuclein in development for treatment of synucleinopathies. Mabs-austin. 2021;13(1):1994690. doi: 10.1080/19420862.2021.1994690.
37. Shah DK, Betts AM. Towards a platform PBPK model to characterize the plasma and tissue disposition of monoclonal antibodies in preclinical species and human. J Pharmacokinet Pharmacodyn. 2012;39(1):67–86. doi: 10.1007/s10928-011-9232-2.
38. Borrok MJ, Wu Y, Beyaz N, X-Q Y, Oganesyan V, Wf D, Tsui P. pH-dependent binding engineering reveals an FcRn affinity threshold that governs IgG recycling. J Biol Chem. 2015;290(7):4282–4290. doi: 10.1074/jbc.M114.603712.
39. Beal S, Sheiner L, Boeckmann A, Bauer R. NONMEM 7.5 User's Guides). NONMEM 7.5 User's Guides. Ellicott City, MD, USA. 1989-2020.
40. Lindbom L, Ribbing J, Jonsson EN. Perl-speaks-NONMEM (PsN)–a perl module for NONMEM related programming. Comput Met Programs Biomed. 2004;75(2):85–94. doi: 10.1016/j.cmpb.2003.11.003.
41. Lindbom L, Pihlgren P, Jonsson EN. PsN-Toolkit–a collection of computer intensive statistical methods for non-linear mixed effect modeling using NONMEM. Comput Met Programs Biomed. 2005;79(3):241–257. doi: 10.1016/j.cmpb.2005.04.005.
42. R Core Team. R: a language and environment for Statistical Computing. Vienna, Austria: R Foundation for Statistical Computing; 2022.
43. RStudio Team. Rstudio: integrated development environment for R. Boston (MA): RStudio, PBC; 2022. http://www.rstudio.com/.
44. Kt B. Mrgsolve: simulate from ODE-Based models [Internet]. 2024; https://mrgsolve.org/docs/.
45. Hooker AC, Staatz CE, Karlsson MO. Conditional weighted residuals (CWRES): a model diagnostic for the FOCE method. Pharm Res. 2007;24(12):2187–2197. doi: 10.1007/s11095-007-9361-x.
46. Karlsson MO, Savic RM. Diagnosing model diagnostics. Clin Pharmacol Ther. 2007;82(1):17–20. doi: 10.1038/sj.clpt.6100241.
47. Mould DR, Upton RN. Basic concepts in population modeling, simulation, and model-based drug development-part 2: introduction to pharmacokinetic modeling methods. CPT Pharmacometrics Syst Pharmacol. 2013;2(4):e38. doi: 10.1038/psp.2013.14.
48. Ménochet K, Yu H, Wang B, Tibbitts J, Hsu C-P, Kamath AV, Richter WF, Baumann A. Non-human primates in the PKPD evaluation of biologics: needs and options to reduce, refine, and replace. A biosafe White Paper MAbs. 2022;14(1):2145997. doi: 10.1080/19420862.2022.2145997.
49. Iwasaki K, Uno Y, Utoh M, Yamazaki H. Importance of cynomolgus monkeys in development of monoclonal antibody drugs. Drug Metab Pharmacokinet. 2019;34(1):55–63. doi: 10.1016/j.dmpk.2018.02.003.

50. Mager DE, Woo S, Jusko WJ. Scaling pharmacodynamics from in vitro and preclinical animal studies to humans. Drug Metab Pharmacokinet. 2009;24(1):16–24. doi: 10.2133/dmpk.24.16.
51. Pardridge WM, Boado RJ, Patrick DJ, ka-Wai Hui E, Lu JZ. Blood-brain barrier transport, plasma pharmacokinetics, and neuropathology following chronic treatment of the rhesus monkey with a brain penetrating humanized monoclonal antibody against the human transferrin receptor. Mol Pharm. 2018;15 (11):5207–5216. doi: 10.1021/acs.molpharmaceut.8b00730.
52. Niewoehner J, Bohrmann B, Collin L, Urich E, Sade H, Maier P, Rueger P, Stracke JO, Lau W, Tissot AC, et al. Increased brain penetration and potency of a therapeutic antibody using a monovalent molecular shuttle. Neuron. 2014;81(1):49–60. doi: 10.1016/j.neuron.2013.10.061.
53. Chang H-Y, Morrow K, Bonacquisti E, Zhang W, Shah DK. Antibody pharmacokinetics in rat brain determined using microdialysis. Mabs-austin. 2018;10(6):843–853. doi: 10.1080/19420862.2018.1473910.
54. Khoury N, Pizzo ME, Discenza CB, Joy D, Tatarakis D, Todorov MI, Negwer M, Ha C, De Melo GL, Sarrafha L, et al. Fc-engineered large molecules targeting blood-brain barrier transferrin receptor and CD98hc have distinct central nervous system and peripheral biodistribution compared to standard antibodies. Nat Commun. 2025;16(1):1822. doi: 10.1038/s41467-025-57108-x.
55. Hui KH, Lam TN. Evaluation of the estimation and classification performance of NONMEM when applying mixture model for drug clearance. CPT Pharmacometrics Syst Pharmacol. 2021;10 (12):1564–1577. doi: 10.1002/psp4.12726.
56. Carlsson KC, Savić RM, Hooker AC, Karlsson MO. Modeling subpopulations with the $MIXTURE subroutine in NONMEM: finding the individual probability of belonging to a subpopulation for the use in model analysis and improved decision making. Aaps J. 2009;11(1):148–154. doi: 10.1208/s12248-009-9093-4.
57. Monine M, Norris D, Wang Y, Nestorov I. A physiologically-based pharmacokinetic model to describe antisense oligonucleotide distribution after intrathecal administration. J Pharmacokinet Pharmacodyn. 2021;48(5):639–654. doi: 10.1007/s10928-021-09761-0.
58. Ogama Y, Kumagai Y, Komatsu N, Araki M, Masubuchi N, Akiyoshi H, Matsuura T, Kirisako H, Kyoya A, Nomura F, et al. Phase 1 clinical trial of PPMX-T003, a novel human monoclonal antibody specific for transferrin receptor 1, to evaluate its safety, pharmacokinetics, and pharmacodynamics. Clin Pharmacol Drug Dev. 2023;12(6):579–587. doi: 10.1002/cpdd.1216.